JOURNAL OF THERMOPHYSICS AND HEAT TRANSFER
Vol. 7, No. 4, Oct.–Dec. 1993

New Two-Temperature Dissociation Model for Reacting Flows

David P. Olynick* and H. A. Hassan†
North Carolina State University, Raleigh, North Carolina 27695

A new two-temperature dissociation model for the coupled vibration-dissociation process is derived from kinetic theory. It is applied for flows undergoing compression. The model minimizes uncertainties associated with the two-temperature model of park. The effects of the model on AOTV-type flowfields are examined and compared with the Park model. Calculations are carried out for flows with and without ionization. When considering flows with ionization, a four-temperature model is employed. For Fire II conditions, the assumption of equilibrium between the vibrational and electron-electronic temperatures is somewhat poor. A similar statement holds for the translational and rotational temperatures. These trends are consistent with results obtained using the direct simulation Monte Carlo (DSMC) method.

Introduction

IT is generally agreed that the dissociation rate of a molecule should be at least a function of the translational-rotational and vibrational temperatures. At present, the exact functional dependence on these temperatures is unknown. However, it is suggested that dissociation preferentially occurs for the high-vibrational states. Thus, the amount of dissociation will decrease if the vibrational temperature is lower than the translational temperature. This concept is known as coupled vibrational-dissociation. The coupled vibration-dissociation process is very important in the region of thermal nonequilibrium after a strong shock. Directly behind the shock, the translational temperature reaches its peak value while vibrational temperature lags, because it takes a finite time to reach its equilibrium value. Therefore, a dissociation model that depends only on the translational temperature will tend to overpredict the amount of dissociation. Dissociation also removes vibrational energy. Thus, the vibrational temperature will be underpredicted if a one-temperature dissociation model is used.

One of the early attempts to study the coupled vibration-dissociation process is the coupled vibration dissociation (CVD) theory of Hammerling et al.[1] The primary assumptions of CVD theory are 1) molecules behave like rotationless harmonic oscillators, 2) the vibrational levels are populated according to a Boltzmann distribution at the vibrational temperature, 3) dissociation from all the vibrational levels are characterized by the same cross section, and 4) the vibrational energy equation is a Landau-Teller equation. This theory gives a dissociation rate that is a function of T and T_v. The expression for this rate is given as follows:

$$\frac{K_f(T, T_v)}{K_f(T)} = \frac{\theta_v}{\theta_d} \frac{1 - \exp(-\theta_d/T_v + \theta_d/T)}{\exp(\theta_v/T_v - \theta_v/T)} \frac{\exp(\theta_v/T_v) - 1}{\exp(\theta_v/T) - 1} \tag{1}$$

where $K_f(T)$ is the one-temperature dissociation rate, θ_v is the characteristic vibrational temperature, and θ_d is the characteristic dissociation temperature. This theory proved inadequate because the vibrational energy removed by dissociation was neglected. In later papers by Treanor and Marrone,[2] the vibrational energy removed by dissociation was included. Treanor and Marrone[3] also accounted for preferential dissociation from the upper vibrational levels. Their theory is known as coupled vibration dissociation vibration (CVDV) theory. Finally, the Landau-Teller equation for the relaxation of the total vibrational energy was abandoned. Instead, researchers determined the vibrational relaxation properties of each vibrational level. This approach was used by Treanor et al.[4] and later by Sharma et al.[5] to study the vibrational population distribution for a relaxation problem. The Park study was undertaken to lend credence to his semi-empirical two-temperature model.[6]

Currently, the two-temperature model of Park is the most widely used model for nonequilibrium problems. At present, there is no analysis that gives a sound theoretical basis for the model. The model replaces the translational temperature in the Arrhenius dissociation rate with an average of the translational-rotational temperature and the vibrational temperature. This gives a forward dissociation rate of the following form:

$$K_f(T, T_v) = CT_a^{\alpha} \exp(-\theta_d/T_a) \tag{2}$$

with

$$T_a = T^{1-q}T_v^q, \qquad 0 \le q \le 1$$

To calibrate his model, Park simulated the AVCO shock tube experiments.[7] The conclusion of his study was that q should be $\frac{1}{2}$. Later work has lead to a modification of this conclusion. It is now thought that q should be about $\frac{3}{10}$. Hartung[8] has shown that radiative heating calculations are extremely sensitive to the choice of q. She showed that for the project Fire conditions, a q value of $\frac{1}{2}$ produced a peak radiative heating value that was double that of choosing q equal to $\frac{3}{10}$.

The uncertainty in the choice of q is the prime motivation of this study. If the value of q has to be adjusted for each problem, then the value of Park's approach as a predictive model is severely diminished. Thus, the goal of this study is the derivation and testing of a new two-temperature model which minimizes the uncertainty of the Park model. The effects of the model are examined for project Fire II conditions and other AOTV-type flows. This type of flowfield is characterized by a large region of thermal nonequilibrium in which the coupled vibration-dissociation process is important. The calculated results are compared with the one-temperature dissociation model and the two-temperature model of Park. The derivation of the new two-temperature model and the cal-

Presented as Paper 92-2943 at the AIAA 27th Thermophysics Conference, Nashville, TN, July 6–8, 1992; received July 22, 1992; revision received Oct. 30, 1992; accepted for publication Dec. 16, 1992.
Copyright © 1992 by the American Institute of Aeronautics and Astronautics, Inc. All rights reserved.

*Research Assistant, Department of Mechanical and Aerospace Engineering. Student Member AIAA.
†Professor, Department of Mechanical and Aerospace Engineering. Associate Fellow AIAA.

culation of AOTV-type flowfields will be discussed in the following sections.

Formulation of the Problem

The two-temperature dissociation model to be presented is derived from kinetic theory considerations. It is designed to revert to the one-temperature dissociation rate when thermal equilibrium is reached. The model takes advantage of the fact that the minimum energy required for dissociation for a molecule in a vibrational state with energy equal to ε_v is $D - \varepsilon_v$, where D is the dissociation energy of the molecule from the ground state. The details of the derivation are as follows:

Consider the reaction

$$AB(v) + M \rightleftarrows A + B + M \tag{3}$$

where v is the vibrational level. The production rate for a vibrational level is given by

$$\frac{dn_v}{dt} = -k_f(T, \varepsilon_v)n_v n_M + k_b(T, \varepsilon_v)n_a n_b n_M \tag{4}$$

where k_f and k_b are the forward and backward rate coefficients, n_v, n_A, n_B, and n_M are the number densities of $AB(v)$, A, B, and M, and T is the translational temperature. If this equation is summed over all the vibrational levels, the following equation is obtained:

$$\frac{dn_{AB}}{dt} = -\sum_v k_f(T, \varepsilon_v)n_v n_M + \sum_v k_b(T, \varepsilon_v)n_A n_B n_M \tag{5}$$

where n_{AB} is the number density for AB. To evaluate the summations in the previous equation k_f, k_b, and n_v must be defined. Based on the results of collision theory,[9] the forward rate k_f can be written as

$$k_f(T, \varepsilon_v) = G(T)\exp[-(D - \varepsilon_v)/kT] \tag{6}$$

where G is some function of T. The backward rate (k_b) is related to the forward rate by detailed balancing.

In order to replace the summation by integration in Eq. (5), the discrete distribution function

$$\frac{n_v}{n_{AB}} = \frac{\exp(-\varepsilon_v/kT_v)}{Q}, \qquad Q = \sum_v \exp(-\varepsilon_v/kT_v) \tag{7}$$

where T_v is the vibrational temperature and Q is the partition function, is first replaced by a continuous distribution. This transformation is accomplished by a standard procedure that makes uses of the Dirac delta function, i.e.

$$\frac{n_v(E_v)}{n_{AB}} = \frac{\exp(-E_v/kT_v)}{Q}\,\delta\left(\frac{E_v}{kT_v} - \frac{\varepsilon_v}{kT_v}\right) \equiv f(E_v, T_v) \tag{8}$$

where δ is the Dirac delta function. To derive a one-term representation of the rate, it is noted that Eq. (8) is well-represented by a Hinshelwood-type distribution,[10] i.e.

$$\frac{n_v}{n_{AB}} = g(E_v, T_v) = \frac{1}{\Gamma(\zeta_v/2)}\left(\frac{E_v}{kT_v}\right)^{(\zeta_v/2)-1}\exp(-E_v/kT_v) \tag{9}$$

provided the quantity ζ_v is chosen as

$$\bar{E}_v = kT_v^2\frac{\partial \ln Q}{\partial T_v} = \frac{1}{2}\zeta_v kT_v \tag{10}$$

Note that

$$n_{AB} = \int n_v\, d\left(\frac{E_v}{kT_v}\right) = \int f(E_v, T_v)\, d\left(\frac{E_v}{kT_v}\right) = \int g(E_v, T_v)\, d\left(\frac{E_v}{kT_v}\right) \tag{11}$$

and Γ is the Gamma function.

Whether one deals with harmonic or anharmonic oscillators, Eq. (10) is used to determine ζ_v. Even when one deals with an anharmonic oscillator, the truncated Q (at the dissociation limit) for a harmonic oscillator gives an excellent estimate of ζ_v.

Applying detailed balancing to Eq. (5), k_f and k_b are related as follows at equilibrium:

$$\frac{k_f(T, \varepsilon_v)}{k_b(T, \varepsilon_v)} = \frac{n_A n_B}{n_v} = \frac{n_A n_B}{n_{AB}g(E_v, T)} = \frac{K_{eq}(T)}{g(E_v, T)} \tag{12}$$

where $K_{eq}(T)$ is the equilibrium constant. Substituting Eqs. (9) and (12) into Eq. (5), and replacing the summation with an integration, the following equation is obtained:

$$\frac{dn_{AB}}{dt} = -n_{AB}n_M\int_0^D k_f(T, E_v)g(E_v, T_v)\, d\left(\frac{E_v}{kT_v}\right) + \frac{n_A n_B n_M}{K_{eq}(T)}\int_0^D k_f(T, E_v)g(E_v, T)\, d\left(\frac{E_v}{kT}\right) \tag{13}$$

Comparing the above equation with the rate equation for the reaction, $AB + M \rightleftarrows A + B + M$, results in the desired dissociation rate for AB. The first integral is the forward dissociation rate

$$K_f(T, T_v) = \int_0^D k_f(T, E_v)g(E, T_v)\, d\left(\frac{E_v}{kT_v}\right) \tag{14}$$

The second integral is $K_f(T, T)$. At equilibrium

$$K_f(T) = K_f(T, T) = AT^\alpha \exp(-D/kT) \tag{15}$$

Finally, to evaluate the integral for $K_f(T, T_v)$ the form given for $k_f(T, \varepsilon_v)$ in Eq. (6) is used. This yields the following expression:

$$\frac{K_f(T, T_v)}{K_f(T, T)} = \frac{\zeta_v/2}{(\alpha D/kT_v)^{\zeta_v/2}}\int_0^{\alpha D/kT_v} x^{(\zeta_v/2)-1}\exp(-x)\, dx = \frac{(\zeta_v/2)}{(\alpha D/kT_v)^{\zeta_2/2}}\,\gamma\left(\frac{\zeta_v}{2}, \frac{\alpha D}{kT_v}\right) \tag{16}$$

where

$$\alpha = 1 - T_v/T$$

and γ is the incomplete gamma function.[11] The incomplete gamma function has a series representation that converges quickly.[12] The algorithm for the gamma function can be successfully vectorized. Thus, overhead for evaluating the above functions is quite modest (less than 5% of cpu per iteration).

Next, the limits for the dissociation rate will be considered. When $\alpha \to 0$ or $T_v \to T$, then $K_f(T, T_v)$ approaches the Arrhenius expression for $K_f(T, T)$. When $\alpha \to 1$, i.e., $T_v/T \to 0$, then $K_f(T, T_v) \to K_f(T, T)$. Two issues must be addressed when considering this limit. The first pertains to the interpretation of the result, and the second pertains to the incubation period. The meaning of the result is that if the

vibrational energy of a molecule is frozen in the ground level, then its dissociation rate is a function of the translational temperature. This interpretation is obtained by examining the form of the forward rate and discrete distribution function given in Eqs. (6) and (7). The result should not be interpreted to mean that the incubation time for dissociation is zero, because the use of a vibrational energy equation insures that the upper vibrational levels are excited over a time scale which is much less than the dissociation time scale. Thus, for a nonequilibrium flow, the limit of $\alpha \rightarrow 1$ is never reached, and an appropriate incubation time for dissociation will be obtained using the present model. This fact is demonstrated in the Results section.

As a comparison, it is worth examining the forward-rate expression of Hammerling et al.[1] and its limiting values. A more careful derivation of Eq. (1) gives

$$\frac{K_f(T, T_v)}{K_f(T)} = \frac{\theta_v}{\theta_d} \frac{1 - \exp(-\theta_d/T_v + \theta_d/T)}{1 - \exp(-\theta_v/T_v + \theta_v/T)} \frac{Q_v(T)}{Q_v(T_v)} \tag{17}$$

where

$$Q_v(T) = \frac{1 - \exp(-\theta_d/T)}{1 - \exp(-\theta_v/T)} \tag{18}$$

When $T_v \rightarrow 0$, $Q_v(T_v) \rightarrow 1$ and

$$\lim_{T_v \rightarrow 0} \frac{K_f(T, T_v)}{K_f(T)} = \frac{\theta_v}{\theta_d} Q_v(T) > 0 \tag{19}$$

Thus, the limit is finite.

Finally, it should be noted that this derivation is only valid for flows undergoing compression. This is because for expanding flows a population inversion of the vibrational levels may occur. Thus, the Hinshelwood distribution function used for the vibrational energy will not be valid. However, if the distribution of vibrational energy were known during the expansion, a derivation of the dissociation rate could be undertaken in the same manner as above.

Physical Modeling

The primary interest of this study is the application of two-temperature models to AOTV-type flowfields. Thus, the computation of these flowfields will be discussed in the following paragraphs.

The governing equations for AOTV flowfields have been presented in a number of sources.[13-15] For this study, the following equations will be solved: global mass, momentum and energy, n species, and rotational, vibrational, and electron-electronic energy. In axisymmetric coordinates, the above set of equations can be written as follows:

$$\frac{\partial \boldsymbol{U}}{\partial t} + \frac{\partial \boldsymbol{F}}{\partial x} + \frac{1}{y} \frac{\partial (y\boldsymbol{G})}{\partial y} = \boldsymbol{W} \tag{20}$$

where

$$\boldsymbol{U} = \begin{bmatrix} \rho \\ \rho_2 \\ \vdots \\ \rho_n \\ \rho u \\ \rho v \\ \rho E_r \\ \rho E_v \\ \rho E_e \\ \rho E \end{bmatrix}$$

$$\boldsymbol{R} = \begin{bmatrix} \rho u \\ \rho_2(u + V_{x2}) \\ \vdots \\ \rho_n(u + V_{xn}) \\ \rho u^2 + p + \tau_{xx} \\ \rho uv + \tau_{xy} \\ E_r u + q_{rx} + \sum_{s=\text{mol}} \rho_s e_{rs} V_{xs} \\ E_v u + q_{vx} + \sum_{s=\text{mol}} \rho_s e_{vs} V_{xs} \\ E_e u + q_{ex} + \sum_{s=\text{elec}} (\rho_s e_{es} V_{xs}) + \rho_e e_{ee} V_x e \\ (E + p + \tau_{xx})u + \tau_{xy} v + q_x + q_{rx} + q_{vx} + \\ \ldots + q_{ex} + \sum_{s=1}^{n} \rho_s h_s V_{xs} \end{bmatrix}$$

$$\boldsymbol{G} = \begin{bmatrix} \rho v \\ \rho_2(v + V_{y2}) \\ \vdots \\ \rho_n(v + V_{yn}) \\ \rho uv + \tau_{xy} \\ \rho v^2 + p + \tau_{yy} \\ E_r v + q_{ry} + \sum_{s=\text{mol}} \rho_s e_{rs} V_{ys} \\ E_v v + q_{vy} + \sum_{s=\text{mol}} \rho_s e_{vs} V_{ys} \\ E_e v + q_{ey} + \sum_{s=\text{elec}} (\rho_s e_{es} V_{ys}) + \rho_e e_{ee} V_y e \\ (E + p + \tau_{yy})v + \tau_{xy} u + q_y + q_{ry} + q_{vy} + \\ \ldots + q_{ey} + \sum_{s=1}^{n} \rho_s h_s V_{ys} \end{bmatrix}$$

$$\boldsymbol{W} = \begin{bmatrix} 0 \\ w_2 \\ \vdots \\ w_n \\ 0 \\ (p - \tau_{\theta\theta})/y \\ Q_{T-r} + \sum_{s=\text{mol}} w_s e_r s \\ Q_{T-v} + Q_{v-e} + \sum_{s=\text{mol}} w_s e_v s \\ Q_{T-e} - Q_{v-e} + Q_{\text{chem}} - p_e \left(\frac{\partial u}{\partial x} + \frac{\partial v}{\partial y} \right) \\ + \sum_{s=\text{elec}} w_s e_{es} \\ 0 \end{bmatrix}$$

In the above equations, $V_{(x,y)s}$ is the diffusion velocity of species s in the x or y direction. $E_{(r,v,e)}$ is the total rotational, vibrational or electron-electronic energy per unit volume. $e_{(r,v,e)s}$ is the rotational, vibrational, or electronic energy per unit mass of species s. w_s is the production rate of species s. The various Q terms are the result of coupling between the various energy modes and the chemistry. The modeling of the various terms in the above equations will be discussed in the following paragraphs.

The rotational modes are assumed to be fully excited. Thus, the rotational energy is given by

$$E_r = \sum_{s=\text{mol}} \rho_s e_{rs}, \qquad e_{rs} = \frac{R_{\text{univ}}}{M_s} T_r = R_s T_r$$

where R_{univ} is the universal gas constant and M_s is the molecular weight of species s. For this study, only translational-

rotational coupling Q_{T-r} was considered. Q_{T-r} is modeled by a Landau-Teller-type expression as follows:

$$Q_{T-r} = \sum_{s=\text{mol}} \rho_s R_s \frac{(T - T_r)}{T_r} \tag{21}$$

where

$$\tau_r = Z_r \tau_c, \qquad \tau_c = (\pi/4)(\mu/p) \tag{22}$$

In the above equation, τ_c is the mean collision time, μ is the mixture viscosity, and Z_r is the ratio τ_r/τ_c. Z_r represents the number of collisions it takes a molecule to reach rotational equilibrium. It can be treated as a constant or as a function of temperature using Parker's formula.[16]

The vibrational energy for each species is obtained using a harmonic oscillator model. Thus, the total vibrational energy is given by

$$E_v = \sum_{s=\text{mol}} \rho_s e_{vs}, \qquad e_{vs} = \frac{R_s \theta_{vs}}{\exp(\theta_{vs}/T_{vs}) - 1} \tag{23}$$

where θ_{vs} is the characteristic vibrational temperature of each species. The translational-vibrational coupling Q_{T-v} is modeled using a Landau-Teller expression as

$$Q_{T-v} = \sum_{s=\text{mol}} \rho_s \frac{e_{vs}(T) - e_{vs}(T_v)}{\tau_{vs}} \tag{24}$$

$$\tau_{vs} = \tau_{sL-T} + \tau_{cs} \tag{25}$$

In the above equation, τ_{sL-T} is a molar-averaged relaxation time for each species based on the Millikan-White formula,[17] and τ_{cs} the high-temperature correction to the Millikan-White formula suggested by Park.[6]

The electron-electronic energy equation is obtained assuming a common electron-electronic energy pool characterized by the temperature T_e as suggested by Park. This assumption is made because the coupling is strong between the electrons and the electronic modes.[13] The electronic energy is the sum of the various electronic energy levels for each species. For this study, the electronic energy of the following species was considered: O_2, N, and O. Thus, the total electron-electronic energy can be written as

$$E_e = \rho_e C_{ve} T_e + \sum_{s=\text{elec}} \rho_s e_{es} \tag{26}$$

where

$$e_{es} = R_s \frac{g_{2s}\theta_{\text{els1}} \exp(-\theta_{\text{els1}}/T_e) + g_{3s}\theta_{\text{els2}} \exp(-\theta_{\text{els2}}/T_e)}{g_{1s} + g_{2s} \exp(-\theta_{\text{els1}}/T_e) + g_{3s} \exp(-\theta_{\text{els2}}/T_e)}$$

In the above equations, C_{ve} is the specific heat of the electrons, g_s and θ_{els} are the degeneracies and characteristic electronic temperatures of the various electronic energy levels, and T_e is the electron-electronic temperature.

The Q source terms for the electronic energy are Q_{T-e}, Q_{v-e}, and Q_{chem}. Q_{T-e} is the source of energy from translational-electron coupling. It represents the energy transferred to the electrons from electron-heavy particle collisions. Q_{v-e} is the source of energy from vibration-electron coupling. It is assumed that only $N_2 - e$ coupling is strong.[13] With this assumption, the term is modeled using a Landau-Teller expression with a relaxation time developed by Lee.[18] Finally, Q_{chem} is the amount of energy lost or gained from electron impact dissociation and ionization.

The shear stresses, heat conduction, and diffusion are modeled as follows. The shear stresses are assumed to be proportional to the first derivatives of the velocities. Therefore, using the Stokes assumption, the shear stresses are given by

$$\tau_{ij} = -\mu\left(\frac{\partial u_i}{\partial x_j} + \frac{\partial u_j}{\partial x_i}\right) - \lambda \frac{\partial u_k}{\partial x_k}\delta_{ij}, \qquad \lambda = -\frac{2}{3}\mu \tag{27}$$

The heat conduction vectors are assumed to be given by the Fourier heat law

$$q_j = -k\frac{\partial T}{\partial x_j}, \qquad q_{rj} = -k_r \frac{\partial T_r}{\partial x_j}$$
$$q_{vj} = -k_v \frac{\partial T_v}{\partial x_j}, \qquad q_{ej} = -k_e \frac{\partial T_e}{\partial x_j} \tag{28}$$

The diffusion velocity of species s is assumed to be governed by Fick's law

$$\rho_s V_{sj} = -\rho D_s \frac{\partial c_s}{\partial x_j} \tag{29}$$

where D_s and c_s are the diffusion coefficient and mass fraction of species s. The transport coefficients for the above equations, μ, k, $k_{(r,v,e)}$, and D_s, are obtained from the cross section data of Yos.[19]

For this study, the following seven chemical reactions were considered:

$$\begin{aligned}
&1)\ N_2 + M \rightleftarrows N + N + M\\
&2)\ O_2 + M \rightleftarrows O + O + M\\
&3)\ NO + M \rightleftarrows N + O + M\\
&4)\ N_2 + O \rightleftarrows NO + N\\
&5)\ NO + O \rightleftarrows O_2 + N\\
&6)\ N + O \rightleftarrows NO^+ + e^-\\
&7)\ N + N \rightleftarrows N_2^+ + e^-
\end{aligned} \tag{30}$$

If ionization is small, then only the first five reactions are considered. The forward rates and equilibrium constants for the above reactions are obtained from the Park reaction set.[14,15]

Results

As discussed above, the vibrational energy expression in this study is assumed to be that appropriate for harmonic oscillators. This defines the energy per unit mass as

$$e_{vs} = \frac{R_s \theta_{vs}}{\exp(\theta_v/T_v) - 1} = \frac{\zeta_v}{2} RT_v \tag{31}$$

Using this expression, a forward dissociation rate can be generated. Figure 1 shows a comparison of the forward dissociation rate for the present model, Park's model, and the Hammerling rate from Eq. (17) as function of T_v/T, which is a measure of the degree of nonequilibrium for a two-temperature model. The figure shows that if the degree of nonequilibrium is not too large the present theory agrees with Park's $T^{0.7}T_v^{0.3}$ model and the Hammerling rate at a temperature of about 10,000 K, and agrees with Park's $T^{0.5}T_v^{0.5}$ model for a high-temperature range. However, the present model is not bracketed by the two Parks models or the Hammerling rate and will range above and below them for higher or lower temperatures.

The final observation drawn from Fig. 1 is the behavior of the three models at the limits of T_v/T, zero, and one. As T_v/T gets small, the dissociation rate using the Park model approaches zero. The present model approaches the one-temperature rate while Hammerling's model approaches a finite value smaller than the one-temperature rate. As T_v/T approaches one, i.e., thermal equilibrium, all models produce identical rates.

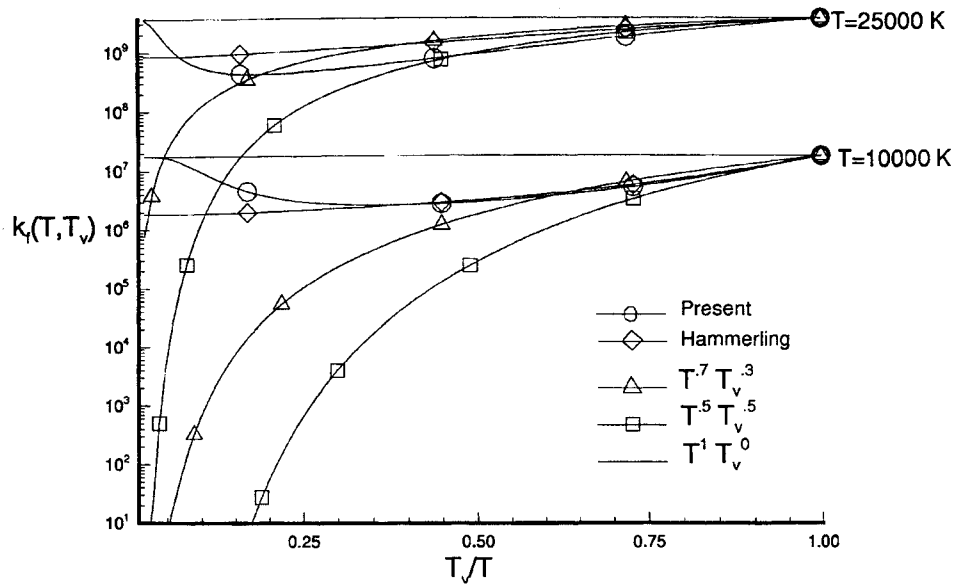

Fig. 1 Comparison of the dissociation rates for the various models.

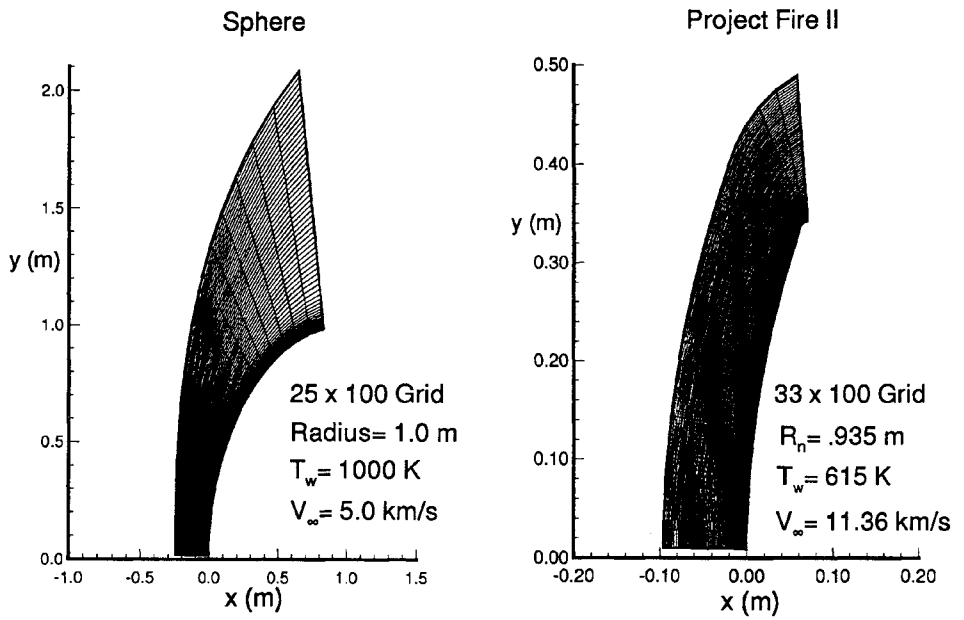

Fig. 2 Geometries for test cases.

To demonstrate the present model, two high-speed flow calculations will be presented. Case 1 is for a 1.0-m radius sphere at 5 km/s with a freestream density of 2.0×10^{-4} kg/m^3 corresponding to an altitude of 63 km. Ionization and the internal electronic modes are neglected and a five-species air model is used. Thus, only two temperatures are considered: a translational-rotational temperature, $T = T_r$, and a vibrational temperature T_v. Case 2 is the 1634 (s) case of project Fire II. The freestream velocity is 11.36 km/s and the density is 3.72×10^{-4} kg/m^3 corresponding to an altitude of 76 km. Both cases considered assume a noncatalytic wall condition and a fixed wall temperature. Figure 2 shows the geometries and grids used in both calculations.

Next, results for the sphere geometry are presented. Figure 3 shows a plot of the translational-rotational and vibrational temperatures along the stagnation line. As expected, the figure shows the two-temperature models produce a higher vibrational and translational temperature. The vibrational temperature of the present model is bracketed by the $T^{0.7}T_v^{0.3}$ and $T^{0.5}T_v^{0.5}$ Park models in the region of moderate thermal nonequilibrium. As thermal equilibrium is approached, all the dissociation models produce similar results. This is consistent with the rates shown in Fig. 1. Finally, directly behind the shock where the thermal nonequilibrium is the largest, all the two-temperature models produce similar results. This is because the amount of dissociation is limited by the low number density.

Next, a number of calculations are generated at the Project Fire II conditions previously stated. In order to compare the results with those for the sphere, the first calculation neglects ionization and the electronic energy modes and a five species air model is used. Again, two temperatures are calculated $T = T_r$ and T_v. Figure 4 shows a plot of these temperatures along the stagnation line in the nonequilibrium region for one temperature dissociation model, a $T^{0.7}T_v^{0.3}$ Park model and the present model. The figure shows the present model results in the highest translational and vibrational temperatures with Park's model in the middle and the T only model producing the lowest temperatures. Again, these results are consistent with the dissociation rates generated in Fig. 1. Figure 5 shows the O_2 and NO mass fractions along the stagnation line. As expected, the two-temperature dissociation models reduce the

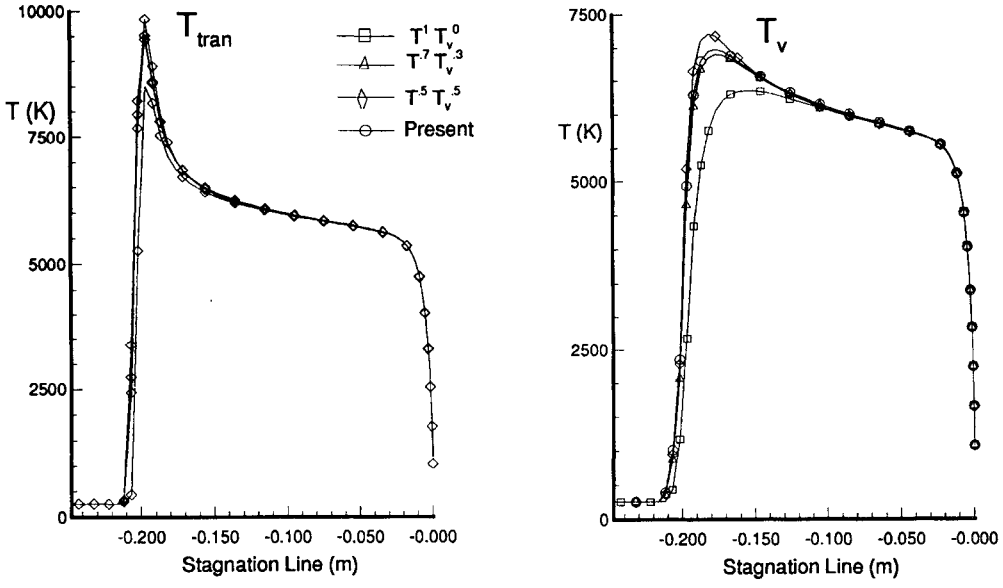

Fig. 3 Translational and vibrational temperatures along the stagnation line for the sphere.

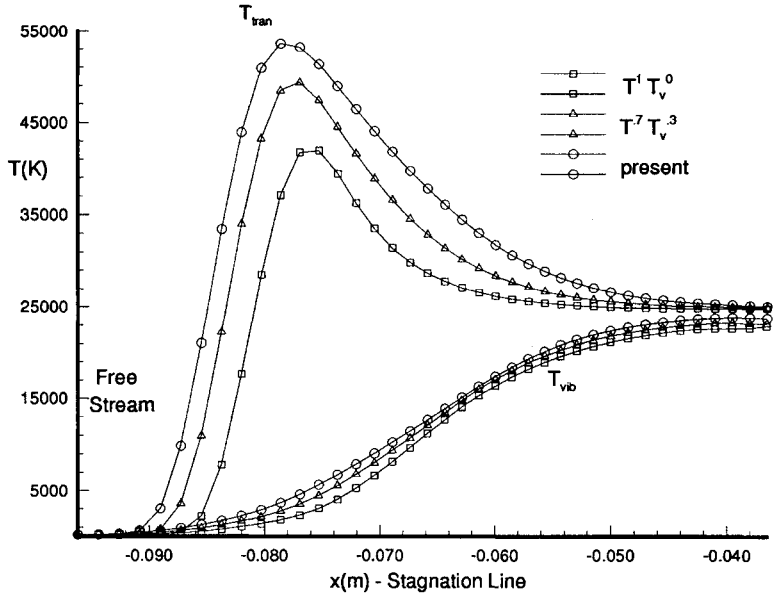

Fig. 4 Translational and vibrational temperatures in the nonequilibrium region for Fire II.

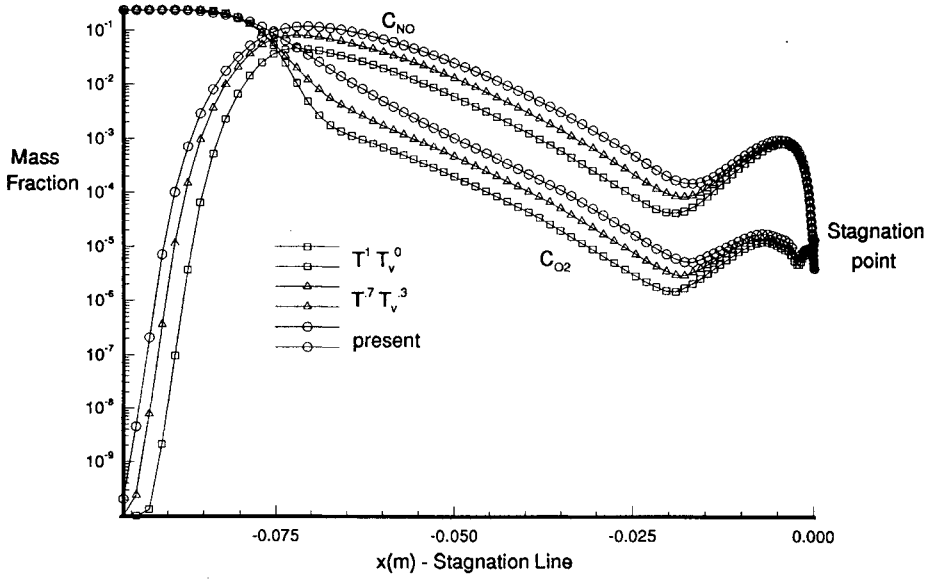

Fig. 5 Mass fractions of O_2 and NO along the stagnation line.

amount of dissociation in the region of thermal nonequilibrium behind the shock. The present model shows the least amount of dissociation and the T only model the most.

The next Fire II calculation includes the effects of ionization and the electronic energy modes. Thus, three temperatures are generated, a translational-rotational temperature, a vibrational temperature, and an electron-electronic temperature. As mentioned in the previous section, the electron and electronic energy are assumed to be a single energy pool characterized by the temperature, T_e. For this case, the eight species reaction model listed in the previous section was used. Figure 6 shows the $T - T_r$ and T_e temperatures along the stagnation line. The plot shows the two-temperature models increase T_e with the present model producing the highest T_e. This behavior is the result of the reduced rate of O_2 dissociation which has a number of low electronic energy states. Figure 7 shows the ion mass fractions along the stagnation line. Since N_2^+ and NO^+ are formed from N-N and N-O collisions, the reduced dissociation rate of the two temperature models reduces the amount of ionization. For N_2^+, the peak ionization is reduced and the location of the peak is shifted towards the body. The lowest ionization peak and the biggest shift occurs for the dissociation model derived in this study. Finally, Fig. 8 shows the vibrational temperatures along the stagnation line. Initially, the two-temperature dissociation models result in a higher vibrational temperature. However, eventually the models cross and the present dissociation model produces the lowest vibrational temperature. The crossover in the temperatures is the result of N_2^+ depletion which at the point of the crossover is largest for the present model.

Finally, the last calculation includes the effects of rotational nonequilibrium. Thus, separate translational, rotational, vibrational, and electron-electronic temperatures are generated. For this calculation, the rotational collision number Z_r, defined in the previous section, is assumed to be a constant of 5. This approach is often used in DSMC calculations. Figure 9 shows T, T_r, T_v, and T_e along the stagnation line for a one-temperature dissociation model and the present two-temperature model. The figure shows the translational temperature is not in equilibrium with rotational temperature and the vibrational temperature is not in equilibrium with the electron-electronic temperature for the various regions of the flow. The trends shown by all the temperatures are consistent with DSMC calculations carried out by Taylor.[20] The behavior of

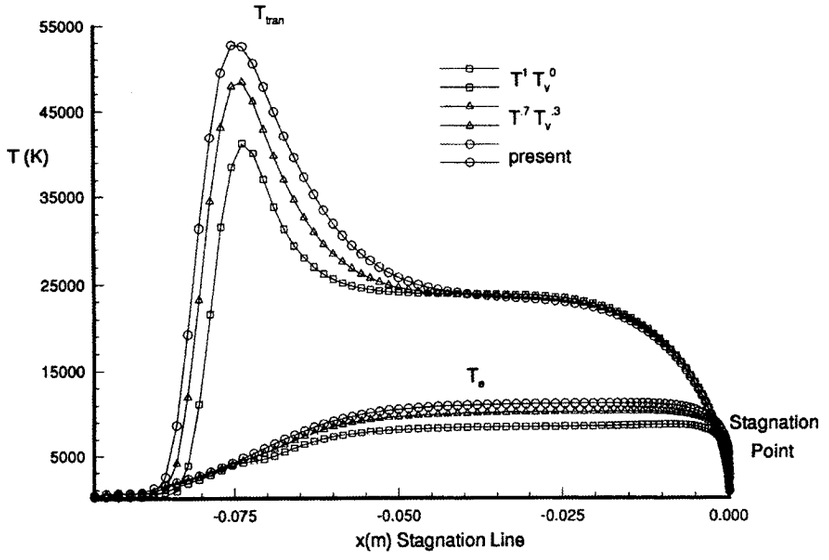

Fig. 6 Translational and electronic temperatures along the stagnation line.

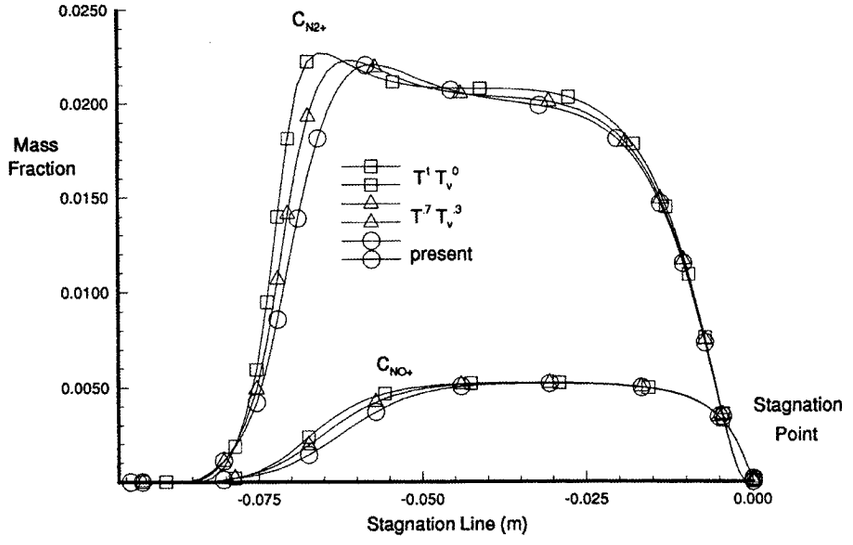

Fig. 7 Ion mass fractions along the stagnation line.

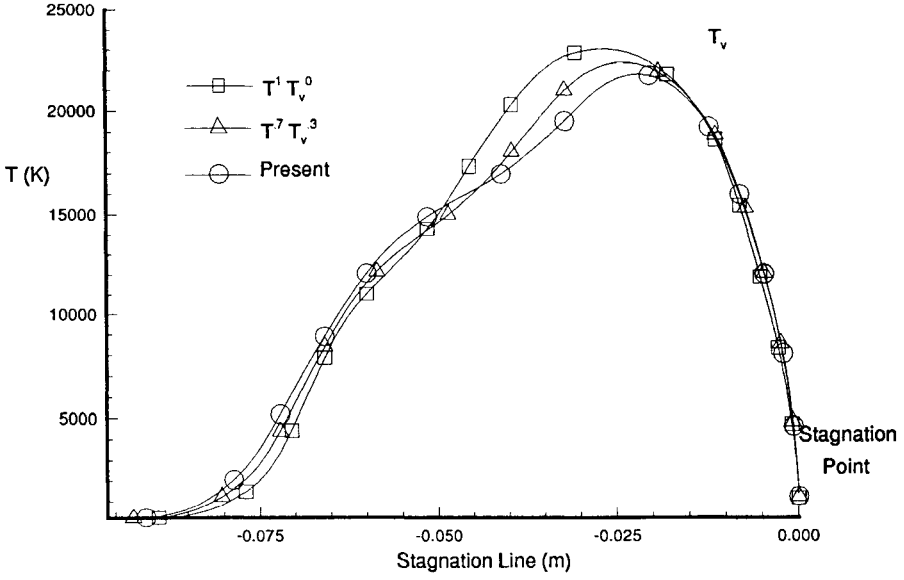

Fig. 8 Vibrational temperature along the stagnation line.

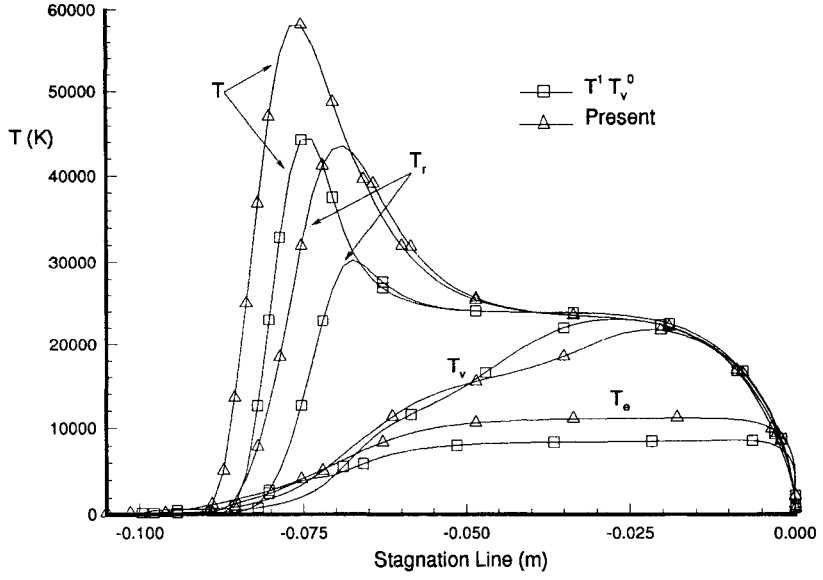

Fig. 9 Temperatures along the stagnation line.

the vibrational and electron-electronic temperatures agrees with the AFE calculations done by Candler.[21] Thus, for Fire II conditions, a two-temperature thermal model may not be a good assumption. Next, the incubation period for the sphere and Fire II calculation is examined.

Figure 10 shows a comparison of T_v/T and the mass fraction of O_2 for the various dissociation models for the sphere calculation. In the figure, T_v/T goes from 1 in the freestream to a minimum value of about 0.25, and again approaches 1 as T_v approaches T along the stagnation line. The incubation period for dissociation occurs around the minimum of T_v/T. In this region, it can be seen that dissociation begins at a similar location for both the present and Park models. Figure 11 shows T_v/T and the mass fractions of O_2 and N_2 along the stagnation line for the previous Fire II calculation. The minimum value of T_v/T is about 0.05 which is much less than the value for the sphere. However, even for this small value of T_v/T, the onset of dissociation is similar for both models. Re-examining Fig. 1, it can be seen that for the higher temperature, the forward rate for the present model does not approach the one-temperature rate until T_v/T is almost zero. The above results also indicate that the forward rate does not

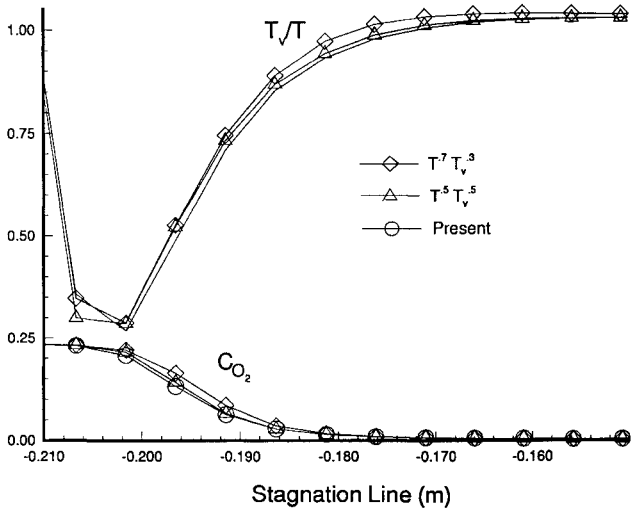

Fig. 10 Comparison of T_v/T and C_{O_2} for the various dissociation models for the sphere.

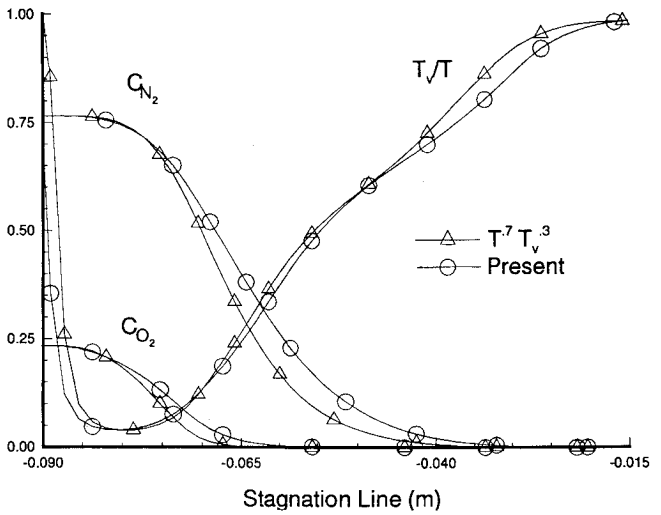

Fig. 11 Comparison of T_v/T and C_{O_2} and C_{N_2} for the various dissociation models for Fire II.

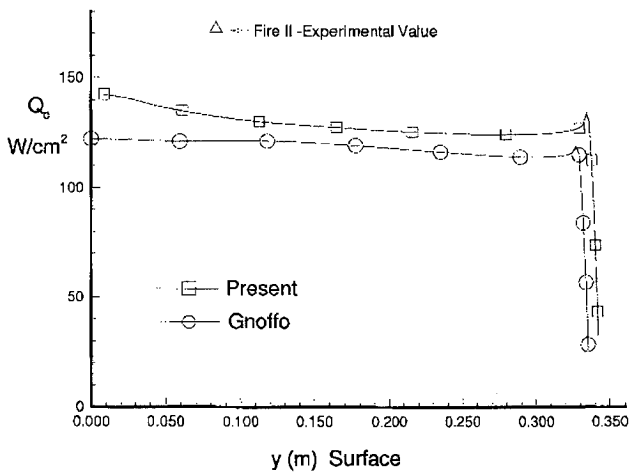

Fig. 12 Surface convective heating for project Fire II.

have to approach zero as T_v approaches zero to arrive at a finite incubation period.

It was found that all models used in the Fire II calculations produced similar convective heat transfer rates. This is expected, since near the body the vibrational temperature equals the translational temperature. Therefore, all the dissociation models give identical dissociation rates. However, the radiative heating is dominated by effects in the nonequilibrium region. Thus, it is expected that the two-temperature models will influence the radiative heat transfer rate. Finally, Fig. 12 shows a comparison of the convective heating along the body for the project Fire calculation assuming a noncatalytic wall condition. The results are compared with the experimental data and calculations of Gnoffo[22] using the latest version of his code. It should be noted that an earlier calculation by Gnoffo[23] for an equivalent sphere geometry of Fire II vehicles showed excellent agreement with the experimental convective heating rates when a fully catalytic wall boundary condition was employed. The plot shows the convective heating is fairly constant along the body. This result is consistent with the experimental data.[24,25] However, the magnitude of the heating is underpredicted.

Conclusions

A new two-temperature model for dissociation is derived from kinetic theory. The model shows a behavior somewhat different from that of Park and minimizes the uncertainties associated with it. Calculations for AOTV-type flows were made with the various two-temperature dissociation models and compared with a one-temperature dissociation model. Calculations with the two-temperature models showed decreased ionization, decreased dissociation, and an increase in the electron-electronic temperature. For Fire II conditions, a two-temperature thermal model was shown to be a poor approximation. Finally, the behavior of the various dissociation models had little effect on the surface convective heat transfer. A comparison with the Fire II experimental data showed the convective heat transfer was underpredicted for a noncatalytic wall condition.

Acknowledgments

This work is supported in part by NASAs Cooperative Agreement NCCI-112; and the Mars Mission Research Center funded by NASA Grant NAGW-1331. Part of the computer time was provided by the North Carolina Supercomputer Center. The authors acknowledge helpful discussions with Peter Gnoffo and Lin Hartung.

References

[1]Hammerling, P., Teare, J. D., and Kivel, B., "Theory of Radiation from Luminous Shock Waves in Nitrogen," *Physics of Fluids*, Vol. 2, No. 4, 1959, pp. 422–426.

[2]Treanor, C. E., and Marrone, P. V., "The Effect of Dissociation on the Rate of Vibrational Relaxation," *Physics of Fluids*, Vol. 5, No. 8, 1962, pp. 1022–1026.

[3]Marrone, P. V., and Treanor, C. E., "Chemical Relaxation with Preferential Dissociation from Excited Vibrational Levels," *Physics of Fluids*, Vol. 6, No. 9, 1963, pp. 1215–1221.

[4]Treanor, C. E., Rich, J. W., and Rehm, R. G., "Vibrational Relaxation of Anharmonic Oscillators with Exchange-Dominated Collisions," *Journal of Chemical Physics*, Vol. 48, No. 4, 1968, pp. 1798–1807.

[5]Sharma, S. P., Huo, W. M., and Park, C., "The Rate Parameters for Coupled Vibration-Dissociation in a Generalized SSH Approximation," AIAA Paper 88-2174, June 1988.

[6]Park, C., "Assessment of a Two-Temperature Kinetic Model for Dissociating and Weakly Ionizing Nitrogen," *Journal of Thermophysics and Heat Transfer*, Vol. 2, No. 1, 1988, pp. 8–16.

[7]Allen, R. A., "Nonequilibrium Shock Front Rotational, Vibrational and Electronic Temperature," AVCO Everett Research Lab., Research Rept. 186, Everett, MA, Aug. 1964.

[8]Hartung, L. C., "Nonequilibrium Radiative Heating Prediction Method for Aeroassist Flowfields with Coupling to Flowfield Solvers," Ph.D. Dissertation, North Carolina State Univ., Raleigh, NC, 1991.

[9]Hansen, C. F., "Rate Processes in Gas Phase," NASA Reference Publication 1090, May 1983.

[10]Hinshelwood, C. N., *The Kinetics of Chemical Change*, Clarendon Press, Oxford, England, UK, 1940, p. 39.

[11]Abramowitz, M., and Stegun, I. A. (eds.), *Handbook of Mathematical Functions*, Dover, New York, 1965, pp. 260–263.

[12]Press, W. H., Flannery, B. P., Teukolsy, S. A., and Vetterling, W. T., *Numerical Recipes: The Art of Scientific Computing*, Cambridge Univ. Press, England, UK, 1986, pp. 160–163.

[13]Park, C., *Nonequilibrium Hypersonic Aerothermodynamics*, Wiley, New York, 1990, pp. 119–143.

[14]Gnoffo, P. A., Gupta, R. N., and Shinn, J. L., "Conservation Equations and Physical Models for Hypersonic Air Flows in Thermal and Chemical Nonequilibrium," NASA TP-2867, Feb. 1989.

[15]Candler, G. V., "The Computation Weakly Ionized Hypersonic Flows in Thermo-Chemical Nonequilibrium," Ph.D. Dissertation, Stanford Univ., Stanford, CA, 1988, pp. 9–32.

[16]Parker, J. G., "Rotational and Vibrational Relaxation in Diatomic Gases," *Physics of Fluids*, Vol. 2, No. 4, 1959, p. 449.

[17]Millikan, R. C., and White, D. R., "Systematics of Vibrational Relaxation," *Journal of Chemical Physics*, Vol. 39, No. 12, 1963, pp. 3209–3213.

[18]Lee, J. H., "Electron-Impact Vibrational Excitation Rates in the Flowfield of AOTV's," *Thermophysical Aspects of Re-Entry Flows*, edited by J. N. Moss and C. D. Scott, Vol. 103, Progress in Aeronautics and Astronautics, 1986, pp. 197–224.

[19]Gupta, R. N., Yos, J. M., Thompson, R. A., and Lee, K. P.,

"A Review of Reaction Rates and Thermodynamic and Transport Properties for an 11-Species Air Model for Chemical and Thermal Nonequilibrium Calculations to 30000 K," NASA Reference Publication 1232, Aug. 1990.

[20]Taylor, J. C., Carlson, A. B., and Hassan, H. A., "Monte Carlo Simulation of Reentry Flows with Ionization," AIAA Paper 92-0493, Jan. 1992.

[21]Candler, G., and Park, C., "The Computation of Radiation from Nonequilibrium Hypersonic Flows," AIAA Paper 88-2678, June 1988.

[22]Gnoffo, P. A., private communication, NASA Langley Research Center, Hampton, VA.

[23]Gnoffo, P. A., "Code Calibration Program in Support of the Aeroassist Fight Experiment," *Journal of Spacecraft and Rockets*, Vol. 27, March–April 1990, pp. 131–142.

[24]Cauchon, D. L., "Radiative Heating Results from the Fire II Flight Experiment at Reentry Velocity of 11.4 Km/s," NASA TM X-1402, July 1967.

[25]Cornette, E. S., "Forebody Temperatures and Calorimeter Heating Rates Measured During Project Fire II Reentry at 11.35 Km/s," NASA TM X-1305, Nov. 1966.

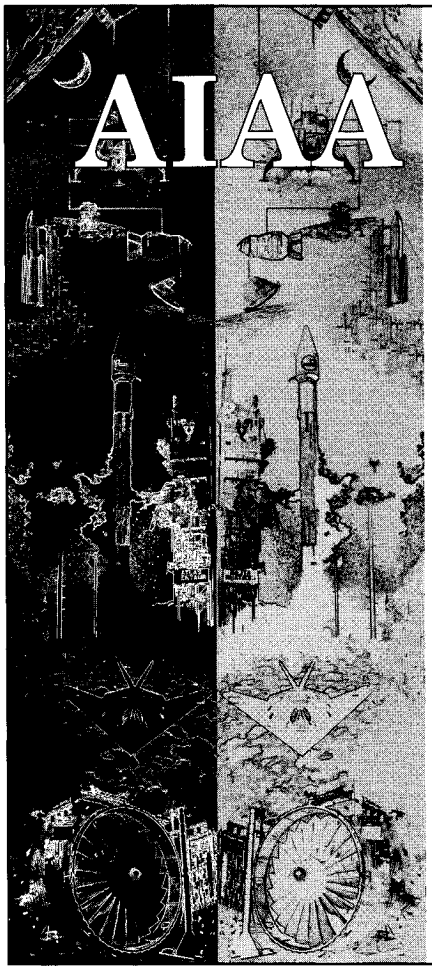

MEMBERSHIP

Technical Information Resources:

- Free subscription to *Aerospace America* with membership
- AIAA Technical Library access
- National and International Conferences
- Book Series: Education Series and Progress in Astronautics and Aeronautics series
- Six Technical Journals: *AIAA Journal, Journal of Aircraft, Journal of Guidance, Control, and Dynamics, Journal of Propulsion and Power, Journal of Spacecraft and Rockets*, and the *Journal of Thermophysics and Heat Transfer*
- Continuing Education Courses

Technical and Standards Committee Membership — Participation in your Profession

Local Activities — *Get to know your peers*

For your convenience an AIAA Membership Application is located in the back of this Journal.

For additional information
contact Leslie Scher Brown
Coordinator, Membership
TEL. 202/646-7430
FAX 202/646-7508

AIAA
American Institute of Aeronautics and Astronautics
370 L'Enfant Promenade, SW
Washington, DC 20024-2518